

Article

Effects of sp^2/sp^3 Ratio and Hydrogen Content on In Vitro Bending and Frictional Performance of DLC-Coated Orthodontic Stainless Steels

Takeshi Muguruma ¹, Masahiro Iijima ^{1,*}, Masahiro Kawaguchi ² and Itaru Mizoguchi ¹

¹ Division of Orthodontics and Dentofacial Orthopedics, School of Dentistry, Health Sciences University of Hokkaido, Hokkaido 061-0293, Japan; muguruma@hoku-iryu-u.ac.jp (T.M.); mizo@hoku-iryu-u.ac.jp (I.M.)

² Surface Coating and Chemical Technology Group, Tokyo Metropolitan Industrial Technology Research Institute, 2-4-10 Aomi Koto-ku, Tokyo 135-0064, Japan; kawaguchi.masahiro@iri-tokyo.jp

* Correspondence: iijima@hoku-iryu-u.ac.jp; Tel.: +81-133-23-2977

Received: 2 April 2018; Accepted: 22 May 2018; Published: 24 May 2018



Abstract: This study investigated a diamond-like carbon (DLC) coating formed on stainless steels (disk and wire specimens) using a plasma-based ion implantation/deposition method with two different parameters (DLC-1, DLC-2). These specimens were characterized using high-resolution elastic recoil analysis, microscale X-ray photoelectron spectroscopy and nanoindentation testing to determine the hydrogen content, sp^2/sp^3 ratio and mechanical properties of the coating. Three-point bending and frictional properties were estimated. DLC-1 had a diamond-rich structure at the external surface and a graphite-rich structure at the inner surface, while DLC-2 had a graphite-rich structure at the external surface and a diamond-rich structure at the inner surface. Mean mechanical property values obtained for the external surface were lower than those for the inner surface in both types of DLC-coated specimens. The hydrogen content of DLC-2 was slightly higher versus DLC-1. Both DLC-coated wires produced a significantly higher elastic modulus according to the three-point bending test versus the non-coated wire. DLC-2 produced significantly lower frictional force than the non-coated specimen in the drawing-friction test. The coating of DLC-1 was partially ruptured by the three-point bending and drawing-friction tests. In conclusion, the bending and frictional performance of DLC-coated wire were influenced by the hydrogen content and sp^2/sp^3 ratio of the coating.

Keywords: diamond-like carbon; frictional property; hydrogen content; surface modification; sp^2/sp^3 ratio

1. Introduction

Metallic orthodontic appliances, such as brackets and archwires, typically show superior properties [1] and provide many clinical advantages, such as low frictional resistance and good bending performance as orthodontic archwires. They have been widely used in clinical orthodontics, although they have esthetic limitations compared to other orthodontic appliances made from ceramics and plastics. Another disadvantage of metallic orthodontic appliances is corrosion in the oral environment [2,3], because the release of metallic ions, such as nickel (Ni) and chromium (Cr), may cause an allergic reaction during orthodontic treatment [4–6].

The frictional force between the bracket and archwire (resistance to sliding) during tooth movement is a primary issue in orthodontics [7,8]. If the frictional force can be decreased, then the efficiency of the tooth movement can be improved. To improve the frictional characteristics and corrosion resistance, various surface modification techniques, such as diamond-like carbon (DLC) coating [9–12], plasma immersion ion implantation [7,13,14] and bioactive glass coating [15], have been investigated.

In recent years, DLC coating has become the subject of considerable research interest due to its bioinertness, extreme hardness, low friction coefficient and high wear resistance [16]. This technique has attracted significant attention for biomedical applications, such as artificial joints, cardiac stents and orthodontic archwires [17]. Concerning orthodontic applications, experimental DLC-coated orthodontic wires have been studied by several research groups [9–12,18–20]. One study reported that DLC layers protect against the diffusion of Ni and its release at the surface of Ni–Ti archwires and that these coatings are noncytotoxic in corrosive environments [18]. Other studies have investigated the effect of DLC coatings on the friction of orthodontic wires and found that DLC-coated wires produced less frictional resistance than non-coated wires [9–12,18–20]. The properties of a DLC coating depend on the hydrogen content, sp^2/sp^3 ratio and presence of doping elements [21,22]. The properties of DLC-coated orthodontic materials are not well understood, and limited information is available regarding the hydrogen content and sp^2/sp^3 ratio of DLC-deposited surfaces.

First, we deposited a DLC film onto orthodontic stainless steels using two different parameters and characterized the DLC films to determine their hydrogen content, sp^2/sp^3 ratio and mechanical properties. The bending and frictional properties of the DLC-coated orthodontic stainless steels were also investigated.

2. Materials and Methods

2.1. Materials

Mechanically-polished stainless steel disk specimens (diameter: 14 mm; thickness: 2 mm; Nogata Denki Kogyo, Tokyo, Japan) and as-received stainless steel orthodontic wires with cross-sectional dimensions of $0.017 \times 0.025 \text{ in}^2$ (stainless steel archwire; 3M Unitek, Monrovia, CA, USA) were purchased and subjected to DLC coating. These stainless steels were confirmed to be Type 304 austenitic stainless steel (ISO No. 4301-304-00-I) by X-ray fluorescence analysis. As-received, preadjusted stainless steel orthodontic brackets (Mini Uni-Twin; 3M Unitek) for the upper canine teeth were used for friction tests. Non-coated specimens served as a control.

2.2. DLC Coating Procedure

DLC films were deposited onto stainless steel disks and wires using a plasma-based ion implantation/deposition (PBIID) method after the specimens were cleaned ultrasonically with acetone and alcohol. A custom-made jig was used to hold the specimens in the PBIID equipment (PEKURIS-HI; Kurita Seisakusho, Kyoto, Japan). To obtain DLC films with different compositions, two different parameters for target voltage, gas atmosphere and deposition time were used; these are listed in Table 1. All deposition processes were carried out at a pressure of $1.33 \times 10^{-3} \text{ Pa}$.

Table 1. Deposition parameters for the DLC coating procedure used in the present study.

DLC Coating Procedure	Target Voltage	Gas Atmosphere	Deposition Time
DLC-1	10 kV	Acetylene + Toluene	3 min
DLC-2	7 kV	Toluene	4 min

2.3. Phase Identification by X-ray Diffraction and Scanning Electron Microscopy of the Coating

Wire specimens were cut into segments (length: 1 cm) using a water-cooled diamond saw (Isomet; Buehler, Lake Bluff, IL, USA). The segments were then placed side-by-side on the sample holder to yield ca. $1 \times 1 \text{ cm}^2$ specimens. Representative surfaces of the control and DLC-coated wire specimens were analyzed using XRD (Rint-2500; Rigaku, Tokyo, Japan) via a parallel-beam method using $\text{Cu-K}\alpha$ radiation (40 kV; tube current: 100 mA) over 2θ ranging from 10° – 60° at a step size of 0.02° and a scan speed of $0.25^\circ \text{ min}^{-1}$. The XRD patterns were obtained at 25° C and analyzed for phase identification

and quantification using PDXL2 software (Rigaku) based on the International Center for Diffraction Data (ICDD) database.

To observe the DLC-coated layers on a cross-sectioned surface, a wire specimen was encapsulated in an epoxy resin (Epofix; Struers, Copenhagen, Denmark) cross-sectioned with a slow-speed, water-cooled diamond saw (Isomet; Buehler) and then ground and polished using a series of silicon carbide abrasive papers and a final slurry of 0.05- μm alumina particles. All specimens were sputter-coated with pure gold for SEM evaluation (JSM-6610LA; JEOL, Tokyo, Japan); the SEM operated at 15 kV.

2.4. Compositional Characterization of the Coating by High-Resolution Elastic Recoil Analysis and Microscale X-ray Photoelectron Spectroscopy

An elastic recoil detection analyzer (ERDA; HRBS1000; Kobelco, Hyogo, Japan) was used for depth profiling of the hydrogen content of DLC-coated disk specimens. The ion type, acceleration voltage, incident angle and scattering angle were N^+ , 500 kV, 67.5 and 45.6°, respectively. The main chamber was maintained at a pressure less than 1×10^{-5} Pa during the measurements. A multi-channel plate was used as the detector in this study. A beam of 500 keV N^+ ions was irradiated against the surface of the specimens, and hydrogen ions recoiled at 45.6° were measured by the 90° sector-type magnetic spectrometer. To reject the scattered N^+ ions, a Mylar foil was set in front of a multi-channel plate detector. The energy of hydrogen ions recoiled from the surface region of the implants was ca. 61 keV. Amorphous carbon materials with 20 at.% hydrogen were used as the standard sample. The standard sample was also measured under the same measurement conditions. The hydrogen contents of the specimens relative to carbon were compared with that of the standard sample. This enabled the depth profile of the contents to be calculated because the change in energy of the hydrogen ions corresponds to their depth from the surface.

The surface and in-depth composition of the control and DLC-coated disk specimens were analyzed by micro-XPS (Quantera II; Ulvac-Phi, Kanagawa, Japan) using $\text{Al K}\alpha$ radiation with a 25-W beam power. The pressure of the main chamber was maintained at less than 1×10^{-6} Pa. Measurements on a 100 μm^2 area of the disk specimens were conducted from 0–1100 eV at a step size of 0.2 eV. The counting time was 20 ms for each step, and the number of sweeps was 5, i.e., the total counting time was 100 ms at each step. Argon-ion sputtering was used for depth profiling measurements. The ion sputtering area was $2 \times 2 \text{ mm}^2$, and the measurements were taken at the center of the area. The sputtering rate of a SiO_2 layer under the same conditions was 13 nm min^{-1} . The sp^2 (for graphite) and sp^3 (for diamond) contents were determined using the software bundled with the XPS apparatus.

2.5. Mechanical Properties of the Coating from Nanoindentation and Three-Point Bending Testing

The external surfaces of DLC-coated wire specimens were examined with a nanoindentation apparatus (ENT-1100a; Elionix, Tokyo, Japan). The specimens were fixed to the specimen stage with adhesive resin (Superbond Orthomite; Sun Medical, Shiga, Japan). Nanoindentation testing was carried out at 28 °C using a Berkovich indenter for depth analyses at 20 and 70 nm ($n = 10$). Linear extrapolation methods (according to the ISO Standard 14577 [23]) were applied to the unloading curve between 95% and 70% of the maximum test force to calculate the elastic modulus. The hardness and elastic modulus of the wire specimen surfaces were calculated using the software bundled with the nanoindentation apparatus.

2.6. Evaluation of the Elastic Modulus of the DLC-Coated Wires by the Three-Point Bending Testing

A three-point bending test was carried out for non-coated and DLC-coated wires ($n = 10$). A 12-mm span was chosen for the wire segments in accordance with the ANSI/ADA Specification No. 32. All samples were loaded following the same protocol on a universal testing machine equipped with a 20 N load cell (EZ Test; Shimadzu, Kyoto, Japan) at room temperature (25 °C). Each wire was first loaded to a deflection of 1.0 or 1.5 mm and then unloaded at a rate of 0.5 mm min^{-1} . Following a

three-point bending test, a specimen was inspected with a stereoscopic microscope (SMZ1500; Nikon, Tokyo, Japan) to observe the detachment of the DLC layers.

2.7. Frictional Properties Measured by the Progressive Load Scratch Test and Drawing Friction Test

A microtribometer (CETR-UMT-2; Bruker, Billerica, MA, USA) was used to characterize the frictional properties of each disk specimen by the progressive-load scratch test. A diamond stylus having a 12.5- μm tip radius was moved 5 mm over a specimen surface with linearly increasing normal load (0.5–20 gf) at a constant speed of 0.016 mm s^{-1} , and the value of the friction coefficient (tangential force) was obtained ($n = 5$). The initial frictional force, average frictional force during the first 0.5-mm scratch and total frictional force and average frictional force during the entire 5-mm scratch were calculated. After the scratch test, each specimen was inspected with a stereoscopic microscope (SMZ1500; Nikon, Tokyo, Japan) to determine the distance for detachment.

The forces generated with each wire/bracket combination were measured under dry and wet (in artificial saliva) conditions at room temperature (25 °C) using a custom-fabricated drawing-friction testing device attached to a universal testing machine (EZ Test; Shimadzu, Kyoto, Japan) [9]. Each bracket was bonded to a stainless steel plate with a non-filled adhesive resin (Superbond; Sun Medical, Shiga, Japan), and a bracket-mounting device provided 10° angular positioning for the bracket. The stainless steel plate with the bracket was attached to a friction-testing device. A 5-cm wire segment was then bound to the bracket using an elastic ligature (Alastik Easy-To-Tie Ligatures, 3M Unitek). The upper end of the wire was fixed to a grip attached to the load cell, and the lower end of the wire was fixed to a 150-g weight. Each wire was drawn through the bracket at a crosshead speed of 10 mm min^{-1} for a distance of 5 mm. The X axis was recorded for wire movement and the Y axis for the force. In the present study, the static frictional force was determined at the initial peak of movement, and the kinetic frictional force was calculated by averaging force values after the static friction peak [7,8]. The sample size for each condition was 10 ($n = 10$). After the drawing-friction test, a specimen was inspected with a stereoscopic microscope (SMZ1500; Nikon) to observe the detachment of the DLC layers.

2.8. Statistical Analyses

Statistical analyses were performed using SPSS Statistics software (ver. 23J for Windows; IBM, Armonk, NY, USA). The mean frictional forces, along with the standard deviation, were analyzed by two-way analysis of variance (ANOVA). The two factors were the coating procedure (non-coating, DLC-1, DLC-2) and test environment (dry, wet). Additionally, the mean hardness, elastic modulus and frictional force were compared using one-way ANOVA, followed by Tukey's or Games–Howell tests. The mean distance for detachment in the progressive-load scratch test was compared using Welch's *t*-test. For all statistical tests, significance was predetermined at $p < 0.05$.

3. Results

3.1. Crystal Structures and Morphological Features of the Coating Layers

Figure 1 displays representative XRD spectra of non-coated and DLC-coated wire specimens. No peak was obtained for either DLC-coated specimen due to their amorphous structures. The XRD spectra for the non-coated wire specimen contained peaks associated with the austenite phase ($\gamma\text{-Fe}$) (ICDD PDF 01-071-4649) and a non-indexed peak at 21.6°.

Representative SEM images of the non-coated and DLC-coated wire specimens are shown in Figure 2. The thin DLC layers on the wire specimen surfaces were ca. 300 nm thick for both the DLC-1 and DLC-2 cases. Good interfacial adhesion was observed between all DLC-deposited layers and bulk materials.

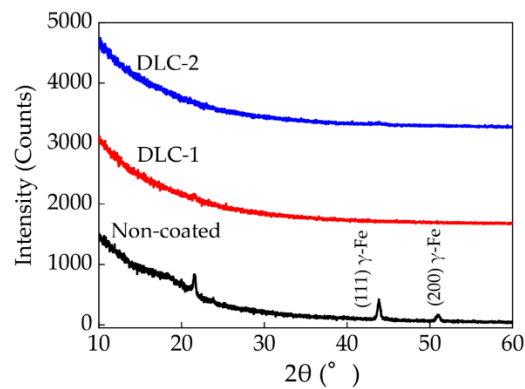


Figure 1. X-ray diffraction patterns obtained from the surfaces of non-coated and diamond-like carbon (DLC)-coated wire specimens.

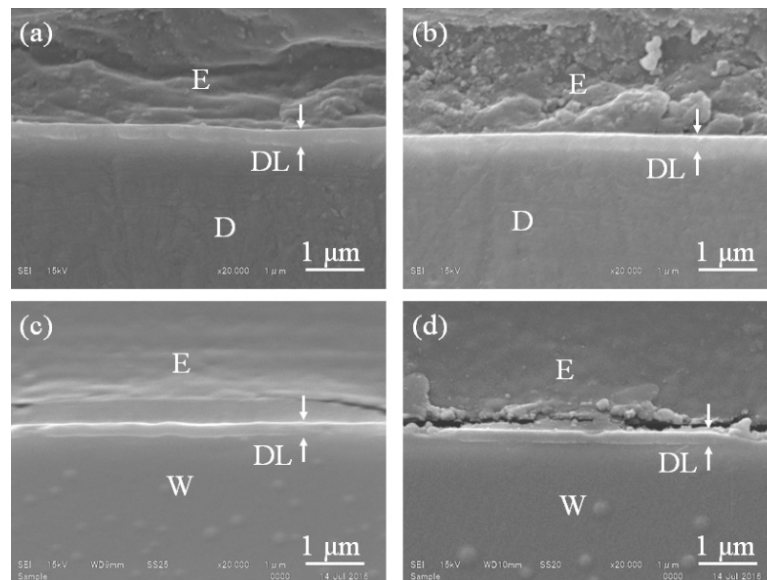


Figure 2. Scanning electron microscopy images of cross-sectioned disk (first row) and wire specimens (second row): (a,c) DLC-coated specimens (DLC-1) and (b,d) DLC-coated specimens (DLC-2). DL, DLC layer; D, disk; W, wire; E, epoxy resin. Original magnification: 20,000 \times .

3.2. Compositional Characterization of the Coating

Figure 3 shows hydrogen depth profile (concentration relative to carbon) by the elastic recoil detection analysis (ERDA) to a depth of 600 Å (60 nm) for the DLC-coated disk specimens. A higher hydrogen concentration was detected for DLC-2. The average hydrogen contents from the top surface to a depth of 600 Å were 23% for DLC-1 and 27% for DLC-2; the external surface regions contained 29% for DLC-1 and 33% for DLC-2.

Figure 4 shows the C 1s spectra obtained by XPS for the DLC-coated disk specimens. Gaussian-Lorentzian curve fitting was used to deconvolute the spectra into three peaks corresponding to sp^2 for graphite-like (284.5 eV) and sp^3 for diamond-like (285.3 eV) and CO-contaminated (283.56–288.43 eV). The amounts of sp^2 and sp^3 and the sp^2/sp^3 ratio (area) for each sputtered layer are summarized in Table 2 (a single layer was ca. 13 nm thick). The C 1s spectra almost disappeared from 40 layers because of the exposure of stainless steel surface to Ar-ion sputtering. The DLC-1 had a higher sp^2/sp^3 ratio (0.343) at the external surface region, although the value decreased (to 0.235) for four sputtered layers, which was similar to that for DLC-2 (0.283). On the other hand, DLC-2 had a

graphite-rich external surface (sp^2/sp^3 ratio: 0.181), although the value increased (to 0.343) after nine sputtered layers, which indicated a diamond-rich surface.

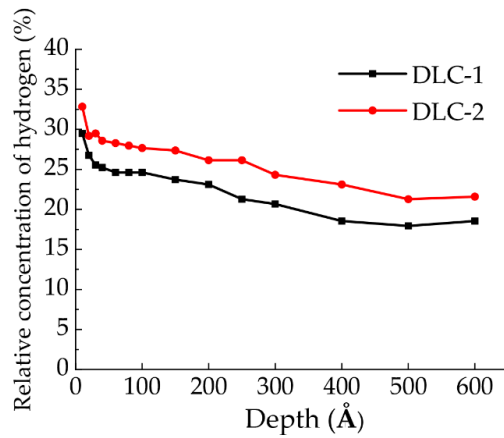


Figure 3. The hydrogen depth profile (concentration relative to carbon) to a depth of 600 Å (60 nm) determined from elastic recoil analyses of DLC-coated disk specimens.

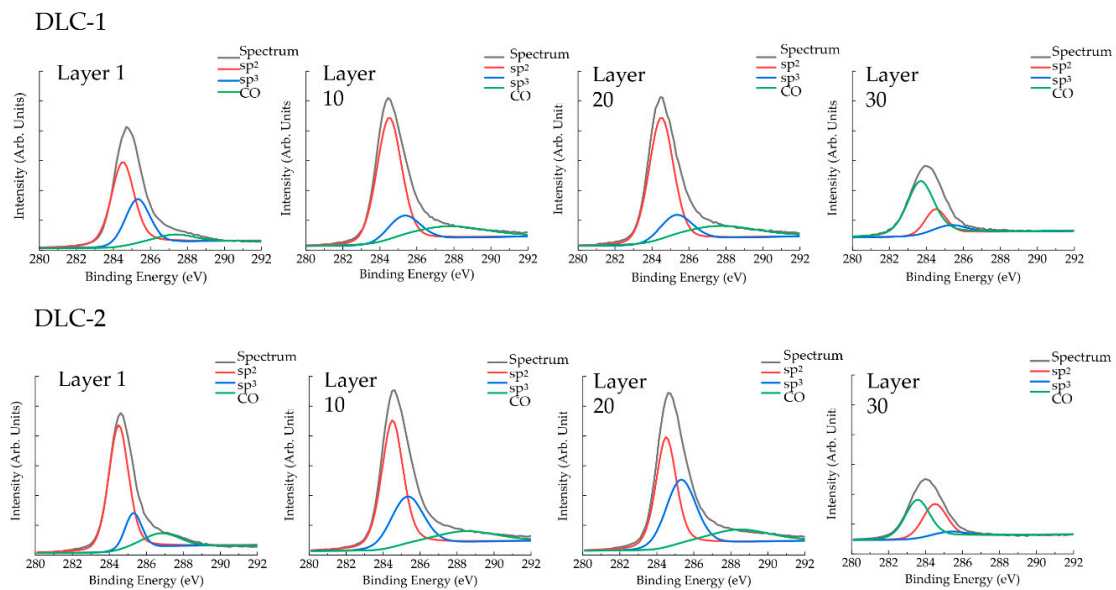


Figure 4. Gaussian-Lorentzian curve fitting of X-ray photoelectron spectroscopy C 1s spectra obtained for DLC-coated disk specimens.

Table 2. The sp^2 , sp^3 and sp^2/sp^3 ratio for each sputtered layer.

Layers	DLC-1			DLC-2		
	sp^2	sp^3	$sp^3/(sp^2 + sp^3)$	sp^2	sp^3	$sp^3/(sp^2 + sp^3)$
1	51,573	26,885	0.343	64,025	14,128	0.181
5	82,776	25,388	0.235	80,737	31,883	0.283
10	78,206	19,654	0.201	73,440	38,368	0.343
15	74,470	20,126	0.213	63,305	45,916	0.420
20	76,467	20,132	0.208	60,451	47,915	0.442
25	73,992	20,656	0.218	71,608	23,626	0.248
30	12,557	6553	0.343	19,183	3356	0.149
35	3864	2553	0.398	911	2221	0.709
40	disappeared	disappeared	–	disappeared	disappeared	–

3.3. Mechanical Properties of the Coating

The mechanical properties of DLC-coated wire specimens obtained from nanoindentation testing at two analysis depths (ca. 20 and 70 nm) are summarized in Table 3. The mean values of the mechanical properties (hardness and elastic modulus) obtained for the external surface regions (at ca. a 20-nm depth) were lower than those for the inner surface regions (at ca. 70 nm depth) for both types of DLC-coated specimens. The DLC-1 tended to show higher mechanical properties at the external surface region and lower mechanical properties at the inner surface region compared with the DLC-2, although only the elastic modulus at the inner surface region was significantly different.

Table 3. Mechanical properties of DLC-coated wires obtained from nanoindentation testing (GPa).

Mechanical Properties	Analysis Depth	DLC-1	DLC-2	<i>p</i> Value ¹
Hardness	20 nm	8.13 (1.24)	7.49 (1.55)	0.317
	70 nm	9.18 (0.64)	9.69 (1.18)	0.241
Elastic modulus	20 nm	117.16 (19.59)	106.35 (36.60)	0.421
	70 nm	123.68 (6.42)	135.40 (12.04)	0.014

Notes: Values are presented as the mean \pm SD; ¹ Student *t*-test.

Table 4 summarizes the elastic modulus for the non-coated and DLC-coated wire specimens obtained by the three-point bending test. Both DLC-coated wires had a significantly higher elastic modulus (181–188 GPa) than the non-coated wire (170 GPa). For the 1.5-mm bending condition, the DLC-1 (188 GPa) had a significantly higher elastic modulus than the DLC-2 (181 GPa). Micrograph images taken following this three-point bending test revealed that the coating layer had been removed from the inner core for both DLC-coated wire specimens; none of the DLC-2 wire coatings were damaged after three-point bending at 1.0 mm (Figure 5).

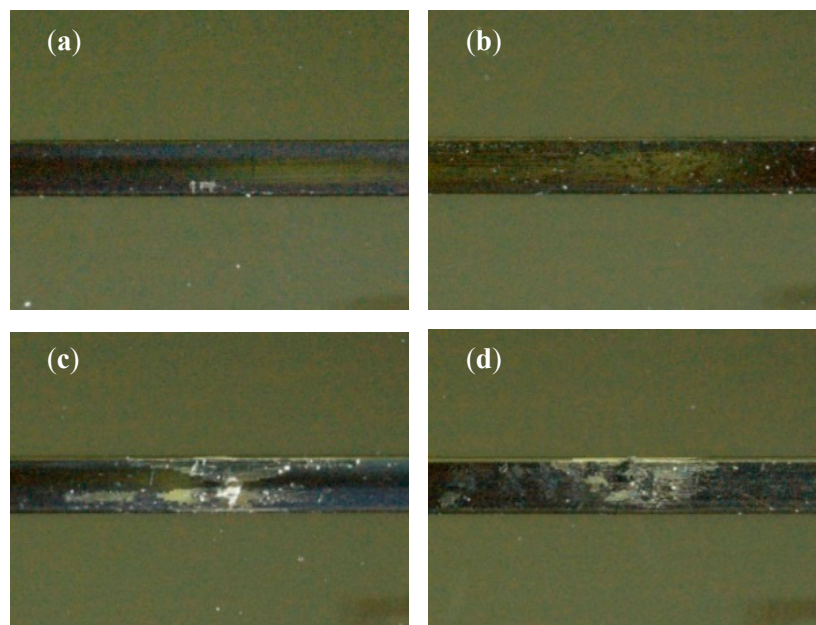


Figure 5. Stereomicroscope images of DLC-coated wires after the three-point bending test. (a,c) DLC-1 and (b,d) DLC-2. The first row shows specimens after the 1.0-mm bending and the second row specimens after the 1.5-mm bending. Original magnification: 50 \times .

Table 4. Elastic modulus for non-coated and DLC-coated wires obtained by the three-point bending test (GPa).

Bending	Non-Coated	DLC-1	DLC-2	p-Value
1 mm	170.45 ^a (1.87)	185.89 ^b (5.85)	181.84 ^b (3.50)	0.000
1.5 mm	170.26 ^a (2.18)	188.42 ^b (4.51)	180.80 ^c (2.54)	0.000

Notes: Values are presented as the mean \pm SD; Identical letters indicate that mean values were not significantly different ($p < 0.05$) by one-way ANOVA followed by the Games–Howell test.

3.4. Frictional Properties Measured by the Progressive Load Scratch Test and Drawing Friction Test

Table 5 summarizes the frictional forces determined by the progressive-load scratch test. Both DLC-coated disk specimens had significantly lower initial and total frictional forces than the non-coated disk specimen. There was no significant difference between the two DLC-coated specimens in terms of the distance for detachment.

Table 5. Frictional forces obtained by the progressive-load scratch test (N).

Scratch Distances	Non-Coated	DLC-1	DLC-2	p-Value
5.0 mm	2.31 ^a (0.02)	2.01 ^b (0.03)	1.97 ^b (0.01)	0.000
0.5 mm	1.20 ^a (0.04)	1.03 ^b (0.07)	0.95 ^c (0.02)	0.000
Distance for detachment (mm)	–	1.05 (0.37)	1.27 (0.20)	0.269 [†]

Notes: Values are presented as the mean \pm SD; Identical letters indicate that mean values were not significantly different ($p < 0.05$) by one-way ANOVA followed by the Tukey multiple test; [†] There was no significant difference between the two DLC-coated specimens in terms of the distance for detachment by Student's *t*-test.

Table 6 summarizes the static and kinetic frictional forces determined from drawing-friction testing of the non-coated and DLC-coated wire specimens under dry and wet conditions. Two-way ANOVA showed that the coating procedure (non-coating, DLC-1, DLC-2) and test environment (dry, wet) were statistically-significant factors affecting both the static and kinetic frictional forces. One-way ANOVA and Tukey's tests showed that the DLC-2 had a significantly lower frictional force than the non-coated specimen, with the exception of the static frictional force under the dry condition. On the other hand, the DLC-1 showed frictional force values that were similar to those of the non-coated specimen, with the exception of the kinetic frictional force under the dry and wet condition. According to the drawing-friction testing, the DLC layers were partially ruptured for the DLC-1 case, while no rupture was observed for the DLC-2 condition (Figure 6).

Table 6. Static and kinetic frictional forces for the non-coated and DLC-coated wires in dry and wet conditions (N).

Friction Test	Condition	Non-Coated	DLC-1	DLC-2	p-Value
Static friction	Wet	2.39 ^a (0.30)	2.37 ^a (0.16)	2.09 ^b (0.22)	0.013
	Dry	2.49 (0.33)	2.47 (0.18)	2.25 (0.24)	0.088
Kinetic friction	Wet	2.37 ^a (0.27)	2.32 ^a (0.17)	1.99 ^b (0.17)	0.001
	Dry	2.55 ^a (0.21)	2.55 ^a (0.30)	2.21 ^b (0.18)	0.004

Notes: Values are presented as the mean \pm SD; Identical letters indicate that mean values were not significantly different ($p < 0.05$) by one-way ANOVA followed by the Games–Howell test.

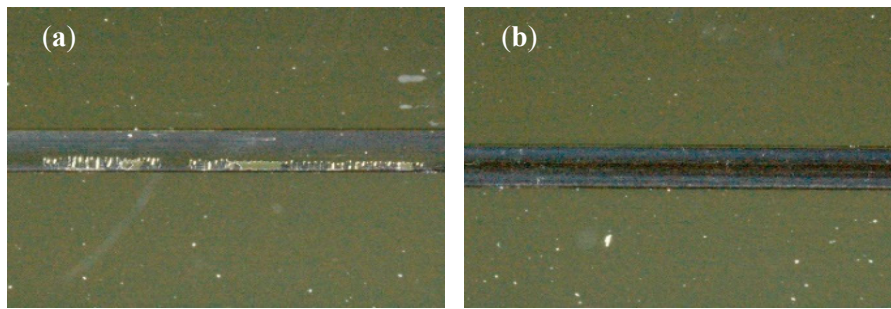


Figure 6. Stereomicroscope images of DLC-coated wires after the drawing-friction test. A portion of the DLC layer had ruptured from the interface. (a) DLC-1 and (b) DLC-2. Original magnification: 50 \times .

4. Discussion

In this study, ca. 300 nm-thick DLC layers were deposited on orthodontic stainless steels. The coatings were amorphous, which was consistent with previous findings [24]. The type of DLC can be identified using a ternary phase diagram [16]. This diagram shows the fraction of carbon sites that have sp^2 (graphite-like) bonding, sp^3 (diamond-like) bonding or bonding with hydrogen. Quantitative analysis of sp^2 and sp^3 bonding in a DLC can be performed by XPS analysis [25,26]. In the present study, the DLC-1 had a higher sp^2/sp^3 ratio (0.343) at the external surface region (ca. 13 nm deep), while the DLC-2 had a lower sp^2/sp^3 ratio (0.181) at the external surface region. This indicated that the external surface of the DLC-1 had a more diamond-rich structure than the DLC-2. After four more layers had been sputtered, the sp^2/sp^3 ratio (measured at a depth of ca. 65 nm) was similar for DLC-1 (0.235) and DLC-2 (0.283). Furthermore, this trend changed after 10 layers were sputtered (measured at a depth of ca. 130 nm) when the DLC-1 displayed a lower sp^2/sp^3 ratio (0.201), although the DLC-2 had a higher sp^2/sp^3 ratio (0.343). This indicated that the inner surface of the DLC-2 had a more diamond-rich structure than the DLC-1. Nanoindentation testing suggested that the DLC-1 had better mechanical properties than the DLC-2 at the external surface region, while the DLC-2 seemed to have better mechanical properties than the DLC-1 at the inner surface region. These findings are supported by the sp^2/sp^3 ratios measured at the different depths in this study, because the diamond structure is harder than the graphite structure [16]. Quantitative analysis of hydrogen in a DLC can be performed by elastic recoil measurements [27]. Using this technique, the average hydrogen content of DLC-2 (27%) was slightly higher than that of DLC-1 (23%). A higher hydrogen content of a DLC coating layer can lead to a higher hardness and elastic modulus [28,29], which may influence wear rate and frictional properties.

Most DLC films are harder than metallic materials. DLC coatings using PBIID methods provide hardnesses ranging from 6 to 20 GPa, depending on the deposition conditions [16,18,19]. The hardness of the DLC layers determined by nanoindentation testing in this study ranged from 9.18 to 9.69 GPa (when measured at a depth of ca. 70 nm), which is much higher than the 6.4 GPa measured by nanoindentation testing under the 20-mN load of the as-received stainless steel orthodontic wire. Additionally, the DLC layers showed a much higher elastic modulus compared with non-coated stainless steel orthodontic wires [30], which should influence the elastic modulus of whole archwires. This is supported by the three-point bending results of the present study. The DLC-coated wire exhibited a significantly higher elastic modulus (by 6%–11% as measured by the three-point bending test) than the non-coated wire. Fortunately, variation of this level may not influence clinical orthodontic tooth movement because a wide range of initial orthodontic forces (18–1500 gf) has been proposed as the optimum force for orthodontic tooth movement, and evidence is lacking regarding the optimal force level [31]. Three-point bending at a span of 1.0 mm caused the coating layer to detach from the inner core for only the DLC-1 wire. None of the coatings of the DLC-2 wires were damaged, probably because the DLC-2 coating had better mechanical properties and adhesion.

Several recent studies of DLC coating reported excellent frictional properties [9–12,18–20], fine cell growth with non-cytotoxicity [18], less bacterial adhesion [32] and inhibited biofilm formation on the metal with DLC coatings [33]. Similarly, the progressive-load scratch test in the present study revealed that both DLC-coated disk specimens (DLC-1, DLC-2) displayed significantly lower frictional forces than the non-coated disk specimens. One explanation for this behavior is that the DLC layer, with higher hardness due to the diamond-rich structure, produced lower frictional forces because of a lower wear rate [16]. Additionally, the hydrogen content might have contributed to lower friction under the dry condition because of the elimination of free σ -bonds on the surface [12]. However, only DLC-2 produced significantly lower frictional force than the non-coated case in the drawing-friction test with a 10° positioning of the bracket under the wet condition. This was attributed to partial rupture of the coating of DLC-1, causing increasing wire-binding at the edge of the bracket [34], thereby increasing the frictional force. Crack initiation and ruptured coating regions were not observed for DLC-2, which suggested that the DLC-2 coating had good flexibility as a functionally-graded material with outstanding adhesion to the orthodontic stainless steel substrate. Additionally, the hydrogen content of the DLC layers might be important under the wet condition. Water molecules might react with a hydrogenated DLC coating to form oxygen-containing hydrophilic groups on the surface that could provide lubrication for the sliding counter surface [21,22]. Another possibility is that hydrogen-terminated surfaces of a hydrogenated DLC coating may interact through weak van der Waals forces [16,22].

The improved frictional properties demonstrated in this work for the DLC-coated samples suggest that tooth movement by sliding mechanics using DLC-coated stainless steel wire may be superior to that using conventional stainless steel wire. However, further randomized controlled trials are required to assess the clinical efficacy.

5. Conclusions

Two types of DLC coatings (DLC-1, DLC-2), differing in hydrogen content, sp^2/sp^3 ratio and mechanical properties, were deposited on orthodontic stainless steel substrates. These coatings affected in vitro bending and frictional properties. DLC-2 showed superior frictional properties, good flexibility and adhesion to the stainless steel. A DLC coating with a higher hydrogen content may provide a better orthodontic wire.

Author Contributions: M.I. conceived of and designed the experiments. T.M., M.I. and M.K. performed the experiments. M.I., T.M. and I.M. wrote the paper.

Funding: This study was partially supported by a Grant-in-Aid Scientific Research from the Ministry of Education, Culture, Sports, Science and Technology, Japan (No. 18K09864).

Acknowledgments: The authors thank Masahiko Sugihara and Yoshimi Nishimura at Kurita Seisakusho for their expert technical assistance with the DLC coating procedure.

Conflicts of Interest: The authors declare no conflict of interest.

References

1. Iijima, M.; Zinelis, S.; Papageorgiou, S.N.; Brantley, W.; Eliades, T. Orthodontic brackets. In *Orthodontic Application of Biomaterials*; Eliades, T., Brantley, W., Eds.; Woodhead Publishing: Sawston, UK, 2017; pp. 75–96.
2. Iijima, M.; Endo, K.; Yuasa, T.; Ohno, H.; Hayashi, K.; Kakizaki, M.; Mizoguchi, I. Galvanic corrosion behavior of orthodontic archwire alloys coupled to bracket alloys. *Angle Orthod.* **2006**, *76*, 705–711. [[PubMed](#)]
3. Bakhtari, A.; Bradley, T.G.; Lobb, W.K.; Berzins, D.W. Galvanic corrosion between various combinations of orthodontic brackets and archwires. *Am. J. Orthod. Dentofac. Orthop.* **2011**, *140*, 25–31. [[CrossRef](#)] [[PubMed](#)]
4. Genelhu, M.C.; Marigo, M.; Alves-Oliveira, L.F.; Malaquias, L.C.; Gomez, R.S. Characterization of nickel-induced allergic contact stomatitis associated with fixed orthodontic appliances. *Am. J. Orthod. Dentofac. Orthop.* **2005**, *28*, 378–381. [[CrossRef](#)] [[PubMed](#)]
5. Amini, F.; Jafari, A.; Amini, P.; Sepasi, S. Metal ion release from fixed orthodontic appliances—An in vivo study. *Eur. J. Orthod.* **2012**, *34*, 126–130. [[CrossRef](#)] [[PubMed](#)]

6. Sifakakis, I.; Eliades, T. Adverse reactions to orthodontic materials. *Aust. Dent. J.* **2017**, *62*, 20–28. [[CrossRef](#)] [[PubMed](#)]
7. Kusy, R.P.; Tobin, E.J.; Whitley, J.Q.; Sioshansi, P. Frictional coefficients of ion-implanted alumina against ion-implanted beta-titanium in the low load, low velocity, single pass regime. *Dent. Mater.* **1992**, *8*, 167–172. [[CrossRef](#)]
8. Burrow, S.J. Friction and resistance to sliding in orthodontics: A critical review. *Am. J. Orthod. Dentofac. Orthop.* **2009**, *135*, 442–447. [[CrossRef](#)] [[PubMed](#)]
9. Muguruma, T.; Iijima, M.; Brantley, W.A.; Mizoguchi, I. Effects of a diamond-like carbon coating on the frictional properties of orthodontic wires. *Angle Orthod.* **2011**, *81*, 141–148. [[CrossRef](#)] [[PubMed](#)]
10. Muguruma, T.; Iijima, M.; Brantley, W.A.; Nakagaki, S.; Endo, K.; Mizoguchi, I. Frictional and mechanical properties of diamond-like carbon-coated orthodontic brackets. *Eur. J. Orthod.* **2013**, *35*, 216–222. [[CrossRef](#)] [[PubMed](#)]
11. Akaike, S.; Hayakawa, T.; Kobayashi, D.; Aono, Y.; Hirata, A.; Hiratsuka, M.; Nakamura, Y. Reduction in static friction by deposition of a homogeneous diamond-like carbon (DLC) coating on orthodontic brackets. *Dent. Mater. J.* **2015**, *34*, 888–895. [[CrossRef](#)] [[PubMed](#)]
12. Zhang, H.; Guo, S.; Wang, D.; Zhou, T.; Wang, L.; Ma, J. Effects of nanostructured, diamondlike, carbon coating and nitrocarburizing on the frictional properties and biocompatibility of orthodontic stainless steel wires. *Angle Orthod.* **2016**, *86*, 782–788. [[CrossRef](#)] [[PubMed](#)]
13. Iijima, M.; Yuasa, T.; Endo, K.; Muguruma, T.; Ohno, H.; Mizoguchi, I. Corrosion behavior of ion implanted nickel-titanium orthodontic wire in fluoride mouth rinse solutions. *Dent. Mater. J.* **2010**, *29*, 53–58. [[CrossRef](#)] [[PubMed](#)]
14. D'Antò, V.; Rongo, R.; Ametrano, G.; Spagnuolo, G.; Manzo, P.; Martina, R.; Paduano, S.; Valletta, R. Evaluation of surface roughness of orthodontic wires by means of atomic force microscopy. *Angle Orthod.* **2012**, *82*, 922–928. [[CrossRef](#)] [[PubMed](#)]
15. Kawaguchi, K.; Iijima, M.; Endo, K.; Mizoguchi, I. Electrophoretic deposition as a new bioactive glass coating process for orthodontic stainless steel. *Coatings* **2017**, *7*, 199. [[CrossRef](#)]
16. Fontaine, J.; Donnet, C.; Erdemir, A. Fundamentals of the tribology of DLC coating. In *Tribology of Diamond-Like-Carbon Films*; Donnet, C., Erdemir, A., Eds.; Springer: New York, NY, USA, 2008; pp. 139–154.
17. Roy, R.K.; Lee, K.R. Biomedical applications of diamond-like carbon coatings: A review. *J. Biomed. Mater. Res. B Appl. Biomater.* **2007**, *83*, 72–84. [[CrossRef](#)] [[PubMed](#)]
18. Kobayashi, S.; Ohgoe, Y.; Ozeki, K.; Hirakuri, K.; Aoki, H. Dissolution effect and cytotoxicity of diamond-like-carbon coating on orthodontic archwires. *J. Mater. Sci. Mater. Med.* **2007**, *18*, 2263–2268. [[CrossRef](#)] [[PubMed](#)]
19. Bentahar, Z.; Barouins, M.; Clin, M.; Bouhammar, N.; Boussirik, K. Tribological performance of DLC-coated stainless steel, TMA and Cu-NiTi. *Int. Orthod.* **2008**, *6*, 335–342. [[CrossRef](#)]
20. Huang, S.Y.; Huang, J.J.; Kang, T.; Diao, D.F.; Duan, Y.Z. Coating NiTi archwires with diamond-like carbon films: Reducing fluoride-induced corrosion and improving frictional properties. *J. Mater. Sci. Mater. Med.* **2013**, *24*, 2287–2292. [[CrossRef](#)] [[PubMed](#)]
21. Okubo, H.; Tsuboi, R.; Sasaki, S. Frictional properties of DLC films in low-pressure hydrogen conditions. *Wear* **2015**, *340*, 2–8. [[CrossRef](#)]
22. Zhang, T.F.; Xie, D.; Huang, N.; Leng, Y. The effect of hydrogen on the tribological behavior of diamond like carbon (DLC) coating sliding against Al₂O₃ in water environment. *Surf. Coat. Technol.* **2017**, *320*, 619–623. [[CrossRef](#)]
23. ISO 14577-1:2002 *Metallic Materials—Instrumented Indentation Test for Hardness and Materials Parameters—Part 1: Test Method*; International Organization for Standardization: Geneva, Switzerland, 2002.
24. Antunes, R.A.; de Lima, N.B.; Rizzutto Mde, A.; Higa, O.Z.; Saiki, M.; Costa, I. Surface interactions of a W-DLC-coated biomedical AISI 316L stainless steel in physiological solution. *J. Mater. Sci. Mater. Med.* **2013**, *24*, 863–876. [[CrossRef](#)] [[PubMed](#)]
25. Tai, F.C.; Lee, S.C.; Wei, C.H.; Tyan, S.L. Correlation between I_D/I_G ratio from visible raman spectra and sp^2/sp^3 ratio from XPS spectra of annealed hydrogenated DLC film. *Mater. Trans.* **2006**, *47*, 1847–1852. [[CrossRef](#)]

26. Ahmed, M.H.; Byrne, J.A.; McLaughlin, J.A.D.; Elhissi, A.; Ahmed, W. Comparison between FTIR and XPS characterization of amino acid glycine adsorption onto diamond-like carbon (DLC) and silicone doped DLC. *Appl. Surf. Sci.* **2013**, *273*, 507–514. [[CrossRef](#)]
27. Torrisi, L.; Cutroneo, M. Elastic recoil detection analysis (ERDA) in hydrogenated samples for TNSA laser irradiation. *Surf. Interface Anal.* **2016**, *48*, 10–16. [[CrossRef](#)]
28. Ronkainen, H.; Varjus, S.; Koskinen, J.; Holmberg, K. Differentiating the tribological performance of hydrogenated and hydrogen-free DLC coatings. *Wear* **2001**, *249*, 260–266. [[CrossRef](#)]
29. Papakonstantinou, P.; Zhao, J.F.; Lemoine, P.; McAdams, E.T.; McLaughlin, J.A. The effects of Si incorporation on the electrochemical and nanomechanical properties of DLC thin films. *Diam. Relat. Mater.* **2002**, *11*, 1074–1080. [[CrossRef](#)]
30. Iijima, M.; Muguruma, T.; Brantley, W.A.; Mizoguchi, I. Comparison of nanoindentation, 3-point bending, and tension tests for orthodontic wires. *Am. J. Orthod. Dentofac. Orthop.* **2011**, *140*, 65–71. [[CrossRef](#)] [[PubMed](#)]
31. Ren, Y.; Maltha, J.C.; Kuijpers-Jagtman, A.M. Optimum force magnitude for orthodontic tooth movement: A systematic literature review. *Angle Orthod.* **2003**, *73*, 86–92. [[PubMed](#)]
32. Muguruma, T.; Iijima, M.; Nagano-Takebe, F.; Endo, K.; Mizoguchi, I. Frictional properties and characterization of a diamond-like carbon coating formed on orthodontic stainless steel. *J. Biomater. Tissue Eng.* **2017**, *7*, 119–126. [[CrossRef](#)]
33. Cazalini, E.M.; Miyakawa, W.; Teodoro, G.R.; Sobrinho, A.S.S.; Matieli, J.E.; Massi, M.; Koga-Ito, C.Y. Antimicrobial and anti-biofilm properties of polypropylene meshes coated with metal-containing DLC thin films. *J. Mater. Sci. Mater. Med.* **2017**, *28*, 97. [[CrossRef](#)] [[PubMed](#)]
34. Muguruma, T.; Iijima, M.; Yuasa, T.; Kawaguchi, K.; Mizoguchi, I. Characterization of the coatings covering esthetic orthodontic archwires and their influence on the bending and frictional properties. *Angle Orthod.* **2017**, *87*, 610–617. [[CrossRef](#)] [[PubMed](#)]



© 2018 by the authors. Licensee MDPI, Basel, Switzerland. This article is an open access article distributed under the terms and conditions of the Creative Commons Attribution (CC BY) license (<http://creativecommons.org/licenses/by/4.0/>).